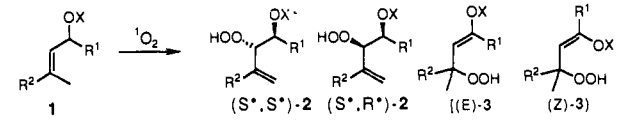


Table I. Regio- and Diastereoselectivity^a in the Photooxygenation^b of Chiral Allylic Acetate **1a** and Alcohols **1b-f**



entry	X	R ¹	R ²	solvent	diastereoselectivity		regio-selectivity		
					(S*,S*)-2 [(E)-3]	(S*,R*)-2 [(Z)-3]	2	3	
1	1a	Ac	Me	Me	CCl ₄	39 [38]	61 [62]	82	18
2	1b	H	Me	Me	CCl ₄	93	7	96	4 ^c
3	1b	H	Me	Me	MeOH ^d	73	27	96	4 ^c
4	1c	H	Me	H	CCl ₄	93	7	>97	<3 ^e
5	1d	H	tBu	H	CCl ₄ ^f	95	5	>97	<3 ^e

^aProduct ratios were determined by ¹H NMR spectroscopy directly in the crude reaction mixture after evaporation of the solvent. ^bUnless otherwise stated, solutions containing 4 mmol of **1** and tetraphenylporphine (TPP) as sensitizer were irradiated with two 150-W sodium lamps at 0 °C while a gentle stream of dry oxygen gas was passed through the solution; full conversion was achieved for **1b** after 4 h, for **1c,d** after 6–8 h, and for **1a** after 9 h. Isolated yields were **2a** 62%, **2b–d** 73–89%. ^cThe regioisomer **3b** was observed in the form of its ring tautomer 3-hydroxy-3,5,5-trimethyl-1,2-dioxolane, produced by ketonization of the initial enol and cyclization. ^dRose bengal was used as sensitizer; 80% conversion after 24 h. ^eNo products from **3c,d** could be detected. ^fThe photooxygenation was conducted in the presence of 10 mol % 2,6-di-*tert*-butyl-4-methylphenol as radical scavenger.

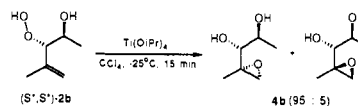
and (*E*)-**3a**. Despite the fact that the chirality center is an inherent part of the reaction coordinate,^{5c,d} diastereofacial discrimination is only moderate because the allylic strain⁷ of the acetoxy group (*erythro* approach) is only slightly smaller than that of the methyl group (*threo* approach).

On the grounds of the *cis* effect,⁵ all of the above was as expected; however, in the photooxygenation of the allylic alcohol **1b** (Table I, entry 2) in CCl₄, not only was a much higher regioselectivity (96:4) and excellent diastereoselectivity (d.r. = 93:7) observed but in the latter case the sense of the stereocontrol was opposite, i.e., *threo* instead of *erythro* attack (Scheme II). The normal *cis* effect⁵ cannot account for the observed selectivities! Instead, we propose coordination of the hydroxy functionality at the chiral allylic site with the incoming ¹O₂ to generate the two diastereomeric peroxide-like transition states *threo*-**1b**^{*} (precursor to the major diastereomer (S*,S*)-**2b**) and *erythro*-**1b**^{*} (precursor to the minor diastereomer (S*,R*)-**2b**). In other words, we are dealing with a novel "cis effect" in which the hydroxy group dictates regio- and diastereocontrol (Scheme II). The *threo* diastereoselectivity dominates because allylic strain⁷ is minimal, i.e., H/H versus H/Me interactions.

Several additional experimental observations support the postulated hydroxy-directing effect. For example, when the photooxygenation of the allylic alcohol **1b** was conducted in methanol (Table I, entry 3), the diastereoselectivity dropped significantly (d.r. = 73:27). Expectedly, hydrogen bonding with methanol provides for less effective stereocontrol by the hydroxy group, and hence the normal *cis* effect⁵ assumes proportionate importance. A similar high degree of diastereoselectivity with predominant formation of the (S*,S*)-configured hydroperoxides is also observed in the photooxygenations of alcohols **1c,d**, in which R¹ groups of different sizes are located at the allylic stereogenic center.

The regio- and diastereoselective oxyfunctionalization of allylic alcohols through the ene reaction with ¹O₂, in which a hydroperoxy functionality is introduced *vicinally* to the existing allylic hydroxy group with both attached to chirality centers, is undoubtedly of synthetic utility. Indeed, when the β-hydroperoxy homoallylic alcohol (S*,S*)-**2b** was submitted to the Ti(OiPr)₄-catalyzed hydroxy epoxidation,⁸ the epoxy diols **4b** (Scheme III) were ob-

Scheme III



tained in high diastereoselectivity (d.r. = 95:5).

In this simple way, two additional chirality centers can be introduced regio- and diastereoselectively in successive adjacent positions to the already existing chiral allylic alcohol moiety. Thus, the present ene reaction of ¹O₂ with chiral allylic alcohols, coupled with the Ti(OiPr)₄-catalyzed hydroxy epoxidation,⁸ constitutes a convenient methodology for multiple oxygenation, in which the novel feature is the directing effect of the chiral allylic hydroxy functionality.

Acknowledgment. The generous financial support by the Deutsche Forschungsgemeinschaft (SFB 347 Selektive Reaktionen Metall-aktivierter Moleküle) and the Fonds der Chemischen Industrie is gratefully appreciated. We thank Dr. A. Griesbeck (Würzburg) for critical but constructive comments.

Supplementary Material Available: Details on the stereochemical assignments (2 pages). Ordering information is given on any current masthead page.

The First *topa*-Containing Copper(II) Complex, [Cu(DL-*topa*)(bpy)(H₂O)]BF₄·3H₂O, as a Model for the Active Site in Copper-Containing Amine Oxidase

Nobuhumi Nakamura, Takamitsu Kohzuma, Hiro Kuma, and Shinnichiro Suzuki*

Institute of Chemistry
College of General Education
Osaka University, Toyonaka, Osaka 560, Japan
Received January 23, 1992

Copper-containing amine oxidases are distributed widely in plants, mammals, and microorganisms. They contain "nonblue" copper and an organic cofactor which is covalently bound to the proteins.¹ In 1984 Duine's² and Ameyama's³ groups independently reported that the covalently bound organic cofactor was pyrroloquinoline quinone (PQQ). However, the evidence for PQQ in copper-containing amine oxidases has not been universally accepted. Recently, *topa* quinone (6-hydroxydopa quinone) residue has been identified as the cofactor in bovine serum amine oxidase.⁴ The cupric site indicated a square pyramidal geometry with three imidazoles and two water molecules.⁵ Dooley and co-workers presented the evidence for the generation of a Cu(I) semiquinone state by room-temperature electron paramagnetic resonance (EPR) measurements and suggested that the Cu(I) semiquinone may be the catalytic intermediate which reacts directly with dioxygen.⁶

* Author to whom correspondence should be addressed.

(1) (a) Knowles, P. F.; Yadav, K. D. S. In *Copper Proteins and Copper Enzymes*; Lontie, R., Ed.; CRC Press: Boca Raton, FL, 1984; pp 103–129. (b) Mondovi, B. In *Structure and Functions of Amine Oxidases*; CRC Press: Boca Raton, FL, 1985. (c) Suzuki, S.; Sakurai, T.; Nakahara, A.; Manabe, T.; Okuyama, T. *Biochemistry* **1983**, *22*, 1630–1635. (d) Suzuki, S.; Sakurai, T.; Nakahara, A.; Manabe, T.; Okuyama, T. *Biochemistry* **1986**, *25*, 338–341.

(2) Lobenstein-Verbeek, C. L.; Jongejan, J. A.; Frank, J.; Duine, J. A. *FEBS Lett.* **1984**, *170*, 305–309.

(3) Ameyama, M.; Hayashi, M.; Matsushita, K.; Shinagawa, E.; Adachi, O. *Agric. Biol. Chem.* **1984**, *48*, 561–565.

(4) Janes, S. M.; Mu, D.; Wemmer, D.; Smith, A. J.; Kain, S.; Maltby, D.; Burlingame, A. L.; Klinman, J. P. *Science* **1990**, *248*, 981–987.

(5) (a) Scott, R. A.; Dooley, D. M. *J. Am. Chem. Soc.* **1985**, *107*, 4348–4350. (b) MaCracken, J.; Peisach, J.; Dooley, D. M. *J. Am. Chem. Soc.* **1987**, *109*, 4064–4072. (c) Dooley, D. M.; McGuirl, M. A.; Cote, C. E.; Knowles, P. F.; Singh, I.; Spiller, M.; Brown, R. D., III; Koenig, S. H. *J. Am. Chem. Soc.* **1991**, *113*, 754–761.

(7) Hoffmann, R. W. *Chem. Rev.* **1989**, *89*, 1841.

(8) Adam, W.; Braun, M.; Griesbeck, A.; Lucchini, V.; Staab, E.; Will, B. *J. Am. Chem. Soc.* **1989**, *111*, 203.

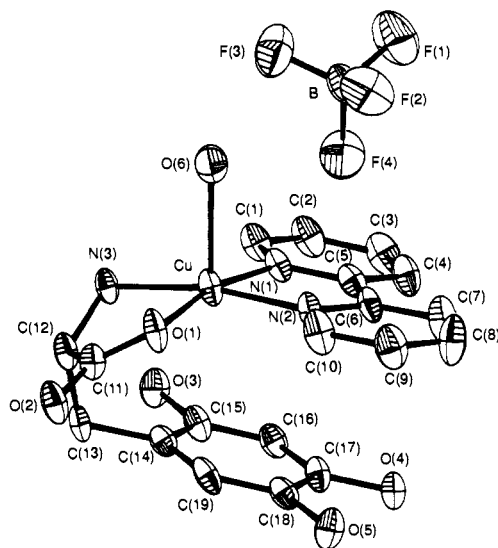


Figure 1. Molecular structure of $[\text{Cu}(\text{DL-topa})(\text{bpy})(\text{H}_2\text{O})]\text{BF}_4 \cdot 3\text{H}_2\text{O}$ (1) showing the 30% probability thermal ellipsoids and atom-labeling scheme. Noncoordinated water molecules and hydrogen atoms are omitted. Selected bond lengths (\AA) and angles (deg) are as follows: Cu–O(1) = 1.946 (8); Cu–O(6) = 2.317 (9); Cu–N(1) = 1.984 (8); Cu–N(2) = 1.981 (8); Cu–N(3) = 2.007 (8); O(3)–C(15) = 1.374 (13); O(4)–C(17) = 1.368 (12); O(5)–C(18) = 1.394 (13); O(1)–Cu–O(6) = 97.1 (3); O(1)–Cu–N(1) = 168.0 (3); O(1)–Cu–N(2) = 91.5 (3); O(1)–Cu–N(3) = 83.3 (4); O(6)–Cu–N(1) = 92.9 (4); O(6)–Cu–N(2) = 92.9 (4); O(6)–Cu–N(3) = 97.3 (4); N(1)–Cu–N(2) = 81.3 (3); N(1)–Cu–N(3) = 102.0 (4); N(2)–Cu–N(3) = 169.1 (4).

In this communication, we report the structure and the catalytic activity of the first topa-containing ternary Cu(II) complex ($[\text{Cu}(\text{DL-topa})(\text{bpy})(\text{H}_2\text{O})]\text{BF}_4 \cdot 3\text{H}_2\text{O}$ (1))⁷ in order to shed light on the structural and the functional relationships between nonblue copper and the organic cofactor in copper-containing amine oxidases.

The complex **1** was prepared according to the following procedures. $[\text{Cu}(\text{bpy})(\text{H}_2\text{O})_2](\text{BF}_4)_2$ (47 μmol) was dissolved in 3 mL of distilled water under Ar atmosphere. DL-topa (47 μmol) was anaerobically added to the solution, and then the mixture was stirred to dissolve topa completely at room temperature. The solution was concentrated to about one-fourth of the volume and permitted to stand at 4 $^\circ\text{C}$ until the bluish green crystals separated out. The crystals suitable for X-ray studies⁸ were obtained by recrystallization from water under Ar atmosphere. topa has two potential chelating sites for a metal ion: the formation of an {N,O} complex with the amino and carboxyl groups and an {O,O} complex with the phenolic dihydroxyl group. The molecular structure of

complex **1** is shown in Figure 1.

In the present synthetic conditions, the {N,O} complex was formed.⁹ The Cu(II) ion has a square pyramidal structure with two nitrogen atoms (N(1) and N(2) numbered according to Figure 1) of bpy and one nitrogen (N(3)) and one oxygen (O(1)) atom of topa coordinated in the equatorial plane and one water oxygen (O(6)) atom occupying a remote axial position. The Cu(II)–O(6) distance, 2.317 (9) \AA , is within the range of axial Cu–O bond lengths (2.2–2.9 \AA).¹⁰ The three nitrogen atoms and one oxygen (O(1)) atom are planar to within experimental error, and the copper atom deviates by 0.17 \AA from the coordination plane (N(1), N(2), N(3), and O(1)) toward the axial oxygen atom (O(6)). The opposite site of the axial O(6) position is occupied by the aromatic ring of the intramolecular topa group, which is approximately parallel to the Cu(II) coordination plane. The closest approach between Cu(II) and the aromatic ring of topa is 3.135 (13) \AA (Cu(II)–C(14)).¹¹ Moreover, the aromatic ring of topa is intramolecularly stacked with the bpy ring. The shortest distance between two rings of topa and bpy is 3.308 (13) \AA (C(15)–N(1)). The dihedral angle between the rings in complex **1** is estimated to be 9.73 $^\circ$. Similar intramolecular stacking is also found in other ternary Cu(II) complexes comprised of aromatic diamines and aromatic amino acids.^{11,12}

An additional noticeable structural feature within a crystal unit is an extensive network of hydrogen-bonding interactions.¹³ The amino and three hydroxyl groups of topa and oxygen atoms of all crystal water molecules are involved in the hydrogen-bonding network. The fluorine atoms (F(1¹) and F(2¹¹))¹⁴ are also located within the hydrogen-bonding distance to the coordinated water oxygen atom (O(6)). The stacking interaction between aromatic rings and the hydrogen-bonding network may play an essential role in stabilizing this crystal structure. X-ray crystallographic analysis of nonblue copper-containing galactose oxidase reveals that the indole ring of Trp is stacked on Tyr, the phenol group of which is coordinated to copper at the active center.¹⁵ The stacking Trp presumably aids stabilization of the free radical. The stacking interaction between the rings of topa and aromatic amino acid residues might also be of consequence at the active sites of amine oxidases.

The oxidation of benzylamine (4.9 mM) with complex **1** (2.4 mM) was carried out in an aqueous solution (pH 7.0) at room temperature under aerobic conditions. After 24 h, the amount of benzaldehyde was determined by HPLC. In comparison with the control reaction with free topa, complex **1** promoted the reaction by a factor of about 14. The $[\text{Cu}(\text{bpy})(\text{H}_2\text{O})_2]^{2+}$ complex shows no oxidation activity of benzylamine. Recently, it has been reported that copper is about 3.0 \AA distant from the C-2 hydroxyl group of topa (O(3) shown in Figure 1) in copper-containing amine oxidase by use of molecular modeling and energy minimization techniques.¹⁶ The distance of 4.073 (8) \AA between copper and

(6) Dooley, D. M.; McGuirl, M. A.; Brown, D. E.; Turowski, P. N.; McIntire, W. S.; Knowles, P. F. *Nature* **1991**, *349*, 262–264.

(7) DL-topa = 3-(2,4,5-trihydroxyphenyl)-DL-alanine; bpy = 2,2'-bipyridine.

(8) Crystal data: $\text{C}_{19}\text{H}_{26}\text{N}_3\text{O}_6\text{BF}_4\text{Cu}$, $M_w = 590.78$; monoclinic, space group $P2_1/a$; $a = 16.259$ (8) \AA , $b = 10.007$ (1) \AA , $c = 16.241$ (4) \AA , $\beta = 114.12$ (3) $^\circ$, $V = 2412$ (1) \AA^3 , $Z = 4$, $D_{\text{calc}} = 1.627$ g cm^{-3} ; $\mu(\text{Cu K}\alpha) = 20.30$ cm^{-1} ; crystal dimensions, $0.10 \times 0.12 \times 0.21$ mm^3 . Intensity data in the range $2\theta < 120^\circ$ were collected by the ω - 2θ scan technique using a Rigaku AFC-5R automated four-circle diffractometer with Ni-filtered Cu K α radiation. Intensities were corrected for Lorentz and polarization effects. An empirical absorption correction based on a series of ψ -scans was applied to the data. The structure was solved by direct methods, MULTAN 78 (Main, P.; Hull, S. E.; Lessinger, L.; Germain, G.; Declercq, J. P.; Woolfson, M. M. *MULTAN 78, A System of Computer Programs for the Automatic Solution of Crystal Structures from X-Ray Diffraction Data*, Universities of York, England, and Louvain, Belgium, 1978), and refined by a block-diagonal least-squares method using the program HBLS-V (Ashida, T. *HBLS-V, The Universal Crystallographic Computing System-Osaka*, The Computation Center, Osaka University, Japan, 1979). Anisotropic temperature factors were used for non-hydrogen atoms. The positions of the hydrogen atoms, except on the water and hydroxyl groups of topa, were calculated on the basis of the molecular geometry. These hydrogen atoms with isotropic temperature factors were included in further refinement. The weighting scheme used was $w = 1/(\sigma(F_o)^2 + 0.3542(F_o) + 0.0002(F_o)^2)$. The final R and R_w values were 0.078 and 0.099 for 2209 reflections ($|F_o| > 3\sigma|F_o|$), respectively.

(9) The electronic absorption and EPR spectra of complex **1** in aqueous solution also indicate that topa coordinates through amino nitrogen and carboxyl oxygen. The absorption spectrum of complex **1** exhibits three peaks at 300 ($\epsilon = 16700$), 314 ($\epsilon = 14300$), and 601 nm ($\epsilon = 104 \text{ M}^{-1} \text{ cm}^{-1}$) at pH 5.2. Many ternary Cu(II) systems comprising bidentate amines and amino acids in aqueous solution exhibit a d–d absorption peak at 580–616 nm in previous study (ref 12b). The EPR spectrum of complex **1** at 77 K shows that the Cu(II) environment is of axial symmetry, displaying the parameters of $g_{\parallel} = 2.24$, $g_{\perp} = 2.06$, and $A_{\parallel} = 18.6$ mT (pH 5.2). Additionally, seven superhyperfine lines ($A_N = 1.2$ mT) due to nitrogens bound to the Cu(II) ion were observed in both the g_{\parallel} and g_{\perp} regions of the signal of complex **1**.

(10) Procter, I. M.; Hathaway, B. J.; Nicholls, P. *J. Chem. Soc. A* **1968**, 1678–1684.

(11) In the ternary Cu(II) complex containing L-tyrosine, $[\text{Cu}(\text{L-tyr})(\text{bpy})(\text{ClO}_4)_2] \cdot 2\text{H}_2\text{O}$, there is a close approach of 3.24 \AA between Cu(II) and the corresponding carbon atom (C(14)) of the phenol ring (Yamauchi, O.; Odani, A.; Masuda, H. *Inorg. Chim. Acta*, in press).

(12) (a) Fischer, B. E.; Sigel, H. *J. Am. Chem. Soc.* **1980**, *102*, 2998–3008. (b) Yamauchi, O.; Odani, A. *J. Am. Chem. Soc.* **1985**, *107*, 5938–5945. (c) Aoki, K.; Yamazaki, H. *J. Chem. Soc., Dalton Trans.* **1987**, 2017–2021. (d) Yamauchi, O.; Odani, A.; Kohzuma, T.; Masuda, H.; Toriumi, K.; Saito, K. *Inorg. Chem.* **1989**, *28*, 4066–4068.

(13) Supplementary material.

(14) Symmetry operations: I $x, -1.0 + y, z$; II $0.5 - x, -0.5 + y, 1.0 - z$.

(15) Ito, N.; Phillips, S. V. E.; Stevens, C.; Ogel, Z. B.; McPherson, M. J.; Keen, J. N.; Yadav, K. D. S.; Knowles, P. F. *Nature* **1991**, *350*, 87–90.

the C-2 hydroxyl oxygen (O(3)) of topa in complex **1** is slightly longer than the above value, but Cu(II) can promote the oxidation of benzylamine. Although these preliminary experiments are not sufficiently extensive to be able to define the mechanism, the finding that Cu(II) is particularly essential for the acceleration of the oxidation of benzylamine is of interest in connection with the mechanism of amine oxidases. Complex **1** might provide significant information on the catalytic roles of the topa residue and copper in copper-containing amine oxidases. Further studies on the spectral and redox properties and the detailed catalytic reaction of complex **1** are in progress.

Acknowledgment. We are very grateful to Prof. Y. Kushi (this Institute), Prof. S. Kaizaki (Faculty of Science, Osaka University), and Prof. O. Yamauchi, Dr. A. Odani, and Dr. H. Masuda (Faculty of Science, Nagoya University) for helpful discussions. This work was supported by a Grant-in-Aid from the Ministry of Education, Science, and Culture, Japan, for Research in Priority Areas (bioinorganic chemistry) (Grant 03241101).

Supplementary Material Available: Figure showing the stereoscopic view of the molecular packing for the complex **1** and tables of positional parameters and isotropic temperature factors for non-hydrogen atoms, interatomic distances and angles, positional parameters and isotropic temperature factors for hydrogen atoms, and anisotropic thermal parameters for non-hydrogen atoms (6 pages); listings of observed and calculated structure factors (9 pages). Ordering information is given on any current masthead page.

(16) McGuirl, M. A.; Brown, D. E.; McCahon, C. D.; Turowski, P. N.; Dooley, D. M. *J. Inorg. Biochem.* 1991, 43, 186.

Novel Tight-Binding Inhibitors of Leukotriene A₄ Hydrolase

Wei Yuan and Chi-Huey Wong*

Department of Chemistry
The Scripps Research Institute
10666 North Torrey Pines Road
La Jolla, California 92037

Jesper Z. Haeggström, Anders Wetterholm, and Bengt Samuelsson*

Department of Physiological Chemistry
Karolinska Institute, Box 60 400
S-104 01, Stockholm, Sweden
Received April 8, 1992

Leukotriene (LT) A₄ hydrolase (EC 3.3.2.6)¹ is a zinc-containing² monomeric enzyme (MW ≈ 70 kDa) which catalyzes the formation of LTB₄ (5(S),12(R)-dihydroxy-6,14-*cis*-8,10-*trans*-eicosatetraenoic acid) from its natural substrate LTA₄ ((5S)-5,6-oxido-7,9-*trans*-11,14-*cis*-eicosatetraenoic acid),^{3,4} one of the

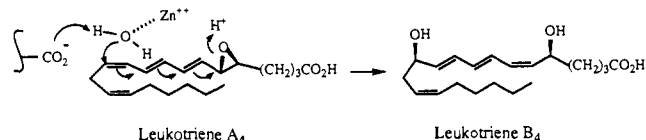
(1) For a review, see: Samuelsson, B.; Funk, C. D. *J. Biol. Chem.* 1989, 264, 19469.

(2) Haeggström, J. Z.; Wetterholm, A.; Shapiro, R.; Vallee, B. L.; Samuelsson, B. *Biochem. Biophys. Res. Commun.* 1990, 172, 965.

(3) Haeggström, J. Z.; Wetterholm, A.; Vallee, B. L.; Samuelsson, B. *Biochem. Biophys. Res. Commun.* 1990, 173, 431. Minami, M.; Ohishi, N.; Mutoh, H.; Izumi, T.; Bito, H.; Wada, H.; Seyama, Y.; Toh, H.; Shimizu, T. *Biochem. Biophys. Res. Commun.* 1990, 173, 620.

(4) Yuan, W.; Zhong, Z.; Wong, C.-H.; Haeggström, J. Z.; Wetterholm, A.; Samuelsson, B. *Biomed. Chem. Lett.* 1991, 1, 551. Several L-amino acid amides such as L-Ala *p*-nitroanilide ($K_m = 0.5$ mM, $V_{max} = 530$ nmol/min/mg enzyme) and L-Pro *p*-nitroanilide ($K_m = 0.1$ mM, $V_{max} = 130$ nmol/min/mg enzyme) are good substrates. The D enantiomers are not substrates. Values of K_m and V_{max} in the ranges 7–30 μ M and 1.7–3.0 μ mol/mg/min, respectively, have been reported using LTA₄ as substrate: Radmark, O.; Haeggström, J. *Adv. Prostaglandin, Thromboxane, Leukotriene Res.* 1990, 20, 35–45. The complementarity components were designed on the basis of computer modeling using MACROMODEL.

Scheme I. Proposed Mechanism for the Hydrolysis of LTA₄ Catalyzed by LTA₄ Hydrolase



Scheme II. Proposed Mechanism for the Aminopeptidase Activity of LTA₄ Hydrolase

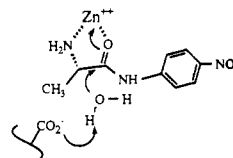


Table I. Inhibitors of LTA₄ Hydrolase

Entry	Compound	IC ₅₀ (μ M) ^a
1		> 100 ^b
2		20
3		80
4		0.5
5		20
6		0.8
7		0.6
8		IC ₅₀ = 0.2 μ M ^c K _i = 0.1 μ M ^c

^a All assays were performed in Tris-HCl buffer (0.05 M, pH 8.0) with L-alanyl *p*-nitroanilide (1.5 mM) as substrate unless otherwise indicated. LTA₄ hydrolase (1.4 μ g) purified from human leukocytes was added for each assay (final volume = 1.0 mL). *p*-Nitroaniline formation was monitored spectrophotometrically at 405 nm. Dixon plot was used to determine the K_i value. ^b Less than 50% inhibition was observed at that concentration. ^c Slow binding behavior was observed. The inhibitor-enzyme mixture was incubated for 30 min prior to addition of the substrate.

physiologically important processes in the arachidonic acid biosynthetic pathway.¹ It also catalyzes the hydrolysis of some L-amino acid amides.^{3,4} The mechanisms of both enzymatic reactions, though not being elucidated, are believed to involve a general base (from a carboxylate) and a Lewis acid (from Zn²⁺) (Schemes I and II). The zinc ion may coordinate to the nucleophilic water molecule to facilitate the general base catalysis. The peptidase and epoxide hydrolase activities, though they occur in the same active site,³ may use a different general base (a carboxylate residue) as indicated in recent site-directed mutagenesis studies.⁵

Since LTB₄ is a proinflammatory mediator which stimulates adhesion of circulating neutrophils to vascular endothelium and directs their migration toward sites of inflammation, it is of interest to develop inhibitors of LTA₄ hydrolase as potential antiinflam-

(5) Haeggström, J. Z.; Samuelsson, B. Unpublished results.